Theoretical investigations of the physical properties of zircon-type YVO$_4$

Zuocai Huang [a], Jing Feng [a,b], Wei Pan [a,*]

[a] State Key Laboratory of New Ceramics and Fine Processing, Department of Materials Science and Engineering, Tsinghua University, Beijing 100084, China
[b] Key Laboratory of Advanced Materials of Precious-Nonferrous Metals, Education Ministry of China, and Key Lab of Advanced Materials of Yunnan Province, Kunming University of Science and Technology, Kunming 650093, China

ARTICLE INFO

ABSTRACT

The crystal structure, electronic properties, elastic properties, hardness and thermodynamic properties of the laser host material zircon-type YVO$_4$ are studied using the pseudopotential plane wave method within the local density approximation (LDA) and generalized gradient approximation (GGA). The calculated ground state values such as lattice parameter, bulk modulus and its pressure derivative, the band structure and densities of states were in favorable agreement with previous works and the existed experimental data. The elastic constants C_{ij}, the aggregate elastic moduli (B, G, E), Poisson's ratio and elastic anisotropy have been investigated. In YVO$_4$, V–O bonds with shorter bond length and larger Mulliken population make great contribution to hardness than Y–O bonds. Using quasi-harmonic Debye model considering the phonon effects, bulk modulus, heat capacity and thermal expansion coefficient of YVO$_4$ are calculated within a range of 0–6 GPa and 0–1200 K.

1. Introduction

Orthovanadates (RVO$_4$, R=trivalent metal) are found to be used in many fields for their great magnetic, optical and electronic properties and they have been widely used as cathodoluminescent materials, scintillators and thermophosphors [1–3]. Recently, diode-pumped solid state lasers have attracted much attention and been widely applied to a number of fields such as military, industry and so on. Among these solid states laser ceramics, YVO$_4$ has been widely investigated [4–6] for its high damage threshold, high conductivity, good mechanical properties and chemical stability, which are important for solid states lasers [7,8]. Other kinds of orthovanadates, such as GdVO$_4$ and ScVO$_4$, have also been studied as laser materials [9,10].

It is well known that thermal conductivity is very important for solid state lasers. The temperature of lasers will rise when energy is released and the efficiency of the laser will come down. What is more, remanent thermal will affect the refractive index, and then result in thermal focusing, stress-induced birefringence. Therefore, the laser output power is limited. As we know, thermal properties depend on mechanical properties of the laser material. Elastic constants, Young's modulus, Poisson' ratio and hardness are very important for laser materials, as well as the anisotropic index of laser materials. In recent years, few efforts have been made to study mechanical and thermal properties from experiments and theoretical calculations [11–15]. Wang et al. [11] studied the structural properties of the zircon-type phase of

YVO$_4$ at high pressure and got the modulus of zircon-type phase of YVO$_4$. Ruju et al. [12] studied the elastic constants of YVO$_4$ single crystal. Zhang et al. [13] studied the thermal and laser properties of Nd:YVO$_4$ crystal and got the thermal expansion and specific heat of Nd:YVO$_4$. Morikawa et al. [14] compared the thermal conductivities of several laser materials including YVO$_4$ by temperature wave analysis. Several studies have reported electronic structure and band gap of YVO$_4$ from experimental and theoretical calculations [15]. The study of material properties such as elastic constants and thermodynamic properties under high temperature and pressure are very important in practical applications, especially for solid state lasers. To our knowledge, there is no systematic report on mechanical and thermodynamic properties of YVO$_4$.

In this paper, we focused on theoretical investigations of the elastic properties, hardness and electronic structure of YVO$_4$ at zero pressure and zero temperature, and also thermodynamic properties at high temperatures and high pressures. Computational methods are described in Section 2. In Section 3, we discussed the calculated mechanical and thermodynamic properties. Finally, a brief summary is given.

2. Computational details and theory

2.1. Computational details

The zircon type phase YVO$_4$ belongs to space group $I4_1/amd$ ($a=b=7.1183$ Å, $c=6.2893$ Å) [16]. The V ions are tetrahedrally coordinated and Y ions are in distorted dodecahedral

* Corresponding author. Fax: +86 10 62771160.
E-mail address: panw@mail.tsinghua.edu.cn (W. Pan).

coordination. The unit cell of the crystal structure is presented in Fig. 1. All calculations of the electronic structure and elastic properties are performed using the pseudo-potential plane-wave method within the framework of the density functional theory and implemented through the Cambridge Serial Total Energy Package (CASTEP) Program [17]. Vanderbilt-type ultra-soft pseudo-potentials [18] are employed to describe the electron–ion interactions ($O2s^22p^4$, $V3s^23p^63d^34s^2$ and $Y4s^24p^64d^15s^2$). Exchange-correlation effects were taken into account using the generalized gradient approximation (GGA) and local density approximation (LDA) as compared. The CA-PZ [19] and PBE [20] functions of the LDA and GGA were chosen, respectively. The plane-wave cutoff energy 600 eV was employed in the calculations. It assured a high level convergence with respect to all parameters: the total-energy difference within 2.0×10^{-5} eV/atom, the maximum Hellmann–Feynaman force within 0.03 eV/Å, the maximum stress within 0.05 GPa and the maximum atom displacement with 1.0×10^{-3} Å. The Brillouin zone sampling was carried out using the $6 \times 6 \times 6$ set of the Monkhost–Pack mesh [21].

2.2. Structural properties

The energy–volume (E–V) curve can be obtained by fitting the calculated E–V data to the third Birch–Murnaghan EOS [22]

$$E(V) = a + bV^{-2/3} + cV^{-4/3} + dV^{-2} \qquad (1)$$

where a, b, c and d are the fitting parameters. To calculate the total energy E and the corresponding volume V, a series of different lattice parameters (a and c) are taken into account. From Table 1, the calculated equilibrium lattice parameters and
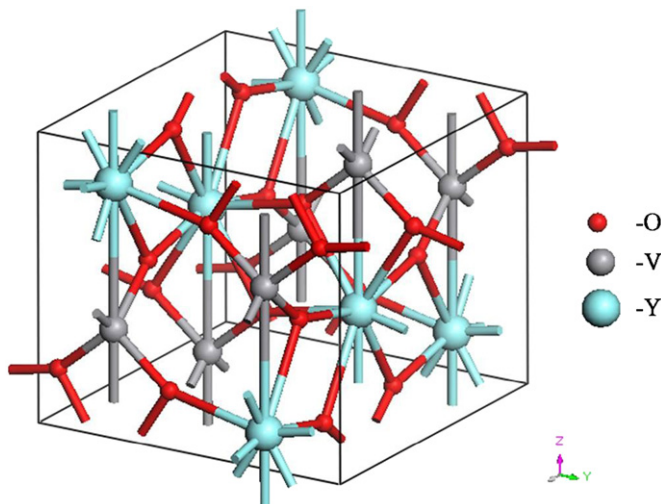

Fig. 1. Crystal structure of zircon-type YVO$_4$ (space group: $I4_1/amd$).

bulk modulus are in good agreement with experimental data [12] and other theoretical results [23], respectively.

The second-order elastic constants were determined by means of linear fitting the stress–strain curves. We applied several different types of Lagrangian strain on crystals and calculated Cauchy stress for each strain after optimizing the internal degrees of freedom. Our calculated elastic constants C_{ij} of YVO$_4$ at zero temperature and zero pressure are listed in Table 1. From Table 1, we can see the calculated elastic constants are in good agreement with experimental values and other calculation results. According to independent elastic constants above, the theoretical polycrystalline elastic modulus can be obtained. There are two approximation methods to calculate the polycrystalline modulus, namely the Voigt method [24] and the Reuss method [25]. The Voigt (B_V) and Reuss (B_R) bulk moduli are given by [26]

$$B_V = (2(C_{11} + C_{12}) + C_{33} + 4C_{13})/9 \qquad (2)$$

$$B_R = C^2/M \qquad (3)$$

The Voigt shear modulus and the Reuss shear modulus are defined as

$$G_V = (M + 3C_{11} - 3C_{12} + 12C_{44} + 6C_{66})/30 \qquad (4)$$

$$G_R = 15/((18B_V)/C^2 + 6/(C_{11} - C_{12}) + 6/C_{44} + 3/C_{66}) \qquad (5)$$

$$M = C_{11} + C_{12} + 2C_{33} - 4C_{13} \qquad (6)$$

$$C^2 = (C_{11} + C_{12})C_{33} - 2C_{13}^2 \qquad (7)$$

The arithmetic average of the Voigt and the Reuss bounds is called the Voigt–Reuss–Hill (VRH) average, which is often used to calculate elastic modulus of polycrystal. The VRH averages for shear modulus (G) and bulk modulus (B) are given by

$$G = (G_R + G_V)/2 \qquad (8)$$

$$B = (B_R + B_V)/2 \qquad (9)$$

Polycrystalline Young's modulus (E), and Poisson's ratio (ν) are then calculated by

$$E = \frac{9BG}{3B + G} \qquad (10)$$

$$\nu = \frac{3B - 2G}{2(3B + G)} \qquad (11)$$

2.3. Thermodynamic properties

In order to investigate thermodynamic properties of YVO$_4$, the quasi-harmonic Debye model [27] is introduced. The quasi-harmonic Debye model has been successfully applied to investigate thermodynamic properties of several materials [28–30]. In the quasi-harmonic Debye model, the non-equilibrium Gibbs

Table 1
Lattice parameters (Å), elastic constants (GPa), bulk modulus (GPa) and their first pressure derivatives of YVO$_4$ calculated by LDA and GGA, along with other theoretical and experimental data.

Method	a	c	B	B'	C_{11}	C_{33}	C_{44}	C_{66}	C_{12}	C_{13}
LDA	7.04	6.195	147.1[a], 145.9[b]	4.1[b]	271.5	337.2	46.4	19.5	54.6	92.1
GGA	7.18	6.314	120.0[a]		216.1	284.8	45.5	21.9	44.3	78.8
Exp. by others[c]	7.118	6.289	130	4.4	244.5	313.7	48.2	16.2	48.93	81.1
Cal. by others[d]	7.05	6.202	142.8		269.0	289.8	46.7	22.3	41.1	79.4

[a] From $B = (2(C_{11} + C_{12}) + C_{33} + 4C_{13})/9$.
[b] From Birch–Murnaghan equation of state.
[c] Ref. [12].
[d] Ref. [23].

function $G^*(V;P,T)$ takes the form of

$$G^*(V;P,T) = E(V) + PV + A_{vib}[\Theta(V);T], \quad (12)$$

where $E(V)$ is the total energy per unit cell, PV corresponds to the constant hydrostatic pressure condition, $\Theta(V)$ is the Debye temperature, and $A_{vib}[\Theta(V);T]$ is the vibrational term, which can be written using the Debye model of the phonon density of states as [31].

$$A_{vib}(\Theta;T) = nkT\left[\frac{9\Theta}{8T} + 3\ln(1-e^{-\Theta/T}) - D\left(\frac{\Theta}{T}\right)\right] \quad (13)$$

where n is the number of atoms per formula unit, $D(\Theta/T)$ represents the Debye integral, which is defined as

$$D(y) = \frac{3}{y^3}\int_0^y \frac{x^3}{e^x-1}dx \quad (14)$$

For an isotropic solid, Θ is expressed as [31]

$$\Theta_D = \frac{h}{k}[6\pi^2 V^{1/2}n]^{1/3}f(\sigma)\sqrt{\frac{B_s}{M}} \quad (15)$$

where M is the molecular mass per unit cell; B_s is the adiabatic bulk modulus, which is approximately given by the static compressibility [27]

$$B_s \cong B(V) = V\frac{\partial^2 E(V)}{\partial V^2} \quad (16)$$

and $f(\sigma)$ is given by Refs. [32,33]; Poisson's σ is taken as 0.336 and 0.318 for LDA and GGA calculations, respectively. Therefore, the non-equilibrium Gibbs function $G^*(V;P,T)$ as a function of $(V;P,T)$ can be minimized with respect to volume V

$$\left[\frac{\partial G^*(V;P,T)}{\partial V}\right]_{P,T} = 0 \quad (17)$$

By solving Eq. (15), one can obtain the thermal equation-of-states (EOS) $V(P,T)$. The heat capacity C_V and the thermal expansion coefficient α are given by [34].

$$C_V = 3nk\left[4D\left(\frac{\Theta}{T}\right) - \frac{3\Theta/T}{e^{\Theta/T}-1}\right] \quad (18)$$

$$S = nk\left[4D\left(\frac{\Theta}{T}\right) - 3\ln(1-e^{-\Theta/T})\right] \quad (19)$$

$$\alpha = \frac{\gamma C_V}{B_T V} \quad (20)$$

where γ is the Grüneisen parameter, which is defined as

$$\gamma = -\frac{d\ln\Theta(V)}{d\ln V} \quad (21)$$

Through the quasi-harmonic Debye model, one could calculate thermodynamic quantities of YVO$_4$ at any temperature and pressure from the calculated E–V data at $T=0$ and $P=0$.

3. Results and discussion

3.1. Electronic properties

The calculated lattice parameters with experimental and theoretical data are shown in Table 1. The calculated results keep in good agreement with the experimental and other theoretical results. And it is known that LDA usually underestimates the lattice constants, while GGA overestimates the lattice constants.

Electronic band structure and density of states often provide sufficient information for a thorough characterization of electronic properties of a material. The energy band structure, total and partial density of states (DOS) of YVO$_4$ were calculated by LDA and GGA. For simplicity, only the results of LDA are presented in

Figs. 2 and 3. The calculated band gap E_g of YVO$_4$ is 3.11 eV, which is very close to other theoretical value of 3.0 eV [35]. But it is smaller than the experimental value of 3.7 eV [36]. Such a discrepancy is expected when the DFT method is used.

From Fig. 3, we can find that the DOS can be mainly divided into four parts. The first part extending from -39.6 eV to -36.5 eV is of the combination of Y s and V p states; The deeper than valence band extending from -20.1 eV to -14.9 eV is of the combination of O s and Y p states; the valence band from -4.9 eV to 0 eV is mainly the contribution of O p states; the conduction band extending from 3.2 eV to 12.5 eV is mainly composed of V d and Y d states.

3.2. Mechanical properties

As is known, elastic constants determine the response of the crystal to external force. For tetragonal crystals, there are six independent elastic constants. The calculated elastic constants of
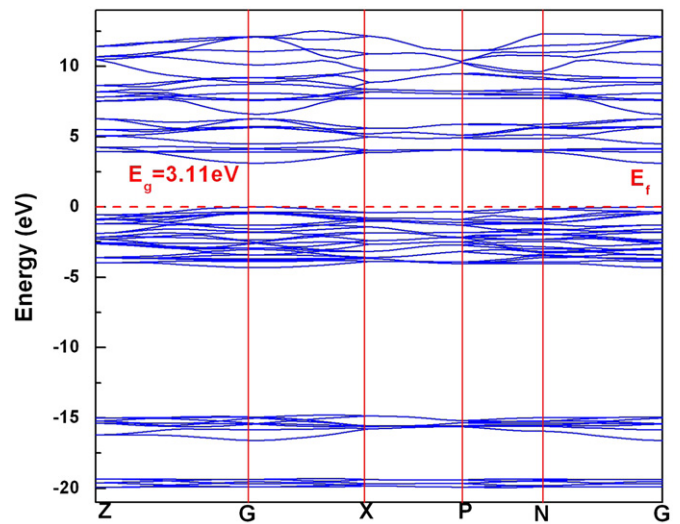

Fig. 2. Energy band structure of zircon-type YVO$_4$ along high symmetry directions in the Brillouin zone. The zero of energy corresponds to the Fermi level.
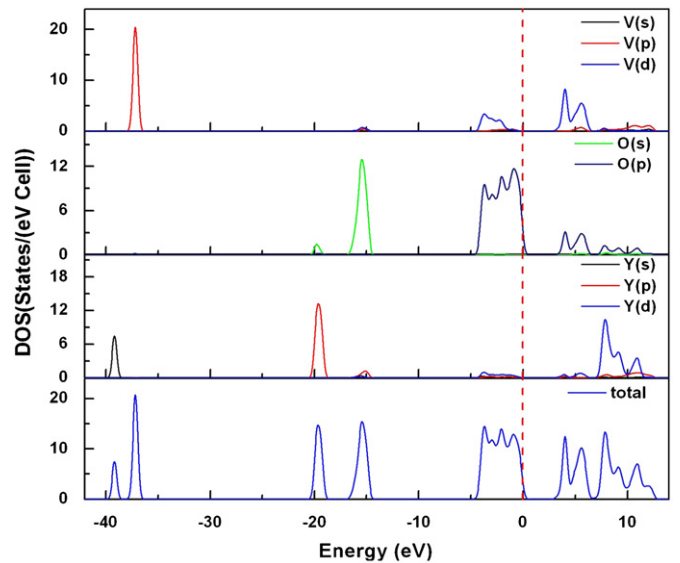

Fig. 3. Calculated partial density of states and total density of states of zircon-type YVO$_4$.

YVO$_4$ are shown in Table 1. It can be seen that elastic constants calculated in this paper keep in good agreement with experimental results [12] and other theoretical values [23]. From Table 1, we can find the results obtained from LDA are higher than the results from GGA. It is known that LDA underestimates the lattice constants and overestimates elastic constants, while GGA overestimates lattice constants and underestimates elastic constants. The mechanical stability criteria for tetragonal YVO$_4$ is

$$(C_{11}-C_{12}) > 0, \quad (2C_{11}+C_{33}+2C_{12}+4C_{13}) > 0, \quad (C_{11}+C_{33}-2C_{13}) > 0,$$

$$C_{11} > 0, \quad C_{33} > 0, \quad C_{44} > 0, \quad C_{66} > 0 \tag{22}$$

The elastic constants in Table 1 satisfy all of these conditions and it indicates that YVO$_4$ is mechanically stable. In present calculations, $C_{11} < C_{33}$, indicating that the bonding strength along [100] and [010] direction is weaker than that of the bonding along [001]. $C_{44} > C_{66}$, suggesting that the [100](010) shear is easier than the [100](001) shear. According to Pugh's criterion [37], the material is supposed to be brittle (ductile), if the B/G value is less (greater) than 1.75. The other condition for being brittle /ductile in nature, derived from Pugh's criterion for B/G is that when v is less than 0.26, the material is brittle, otherwise it is ductile. From Table 2, B/G is 2.72 and v is 0.34, so zircon-type YVO$_4$ is ductile. Compared with single crystal mechanical properties, polycrystalline mechanical properties (such as bulk modulus, shear modulus, Young's modulus and Poisson's ratio) usually have higher practical application value. Using the Voigt–Reuss–Hill approximation [26], those properties were obtained from elastic constants of YVO$_4$ single crystal and listed in Table 2.

It is well known that microcracks are easily induced in the materials due to the significant elastic anisotropy [38]. Therefore, it is important to calculate the elastic anisotropy in order to improve their mechanical durability. From the crystal structure of YVO$_4$, one could suppose that it has high anisotropy. Some researchers have done many studies on this aspect and want to introduce a universal index to describe elastic anisotropy of different types of crystals. Zener [39] first introduced an anisotropy index to quantify the elastic anisotropy of single crystals, but it is just applicable to cubic crystals. In order to quantify the anisotropy of all kinds of elastic single crystals, Shivakumar and Martin [40] introduced universal elastic anisotropy index A^U for all elastic single crystals

$$A^U = 5\frac{G^V}{G^R} + \frac{B^V}{B^R} - 6 \tag{23}$$

where G and B are the shear modulus and bulk modulus, respectively; V and R represent the Voigt and Reuss estimations for B and G, respectively. A^U is identically zero for a locally isotropic single crystal. The departure of A^U from zero defines the extent of single crystal anisotropy and account for both the shear and the bulk modulus contribution unlike all other existing anisotropy measures. For YVO$_4$, $A^U = 2.41$, which means YVO$_4$ is anisotropic [40].

Furthermore, a three-dimensional (3D) curved surface, representing the dependence of elastic properties on crystallographic directions, can indicate the elastic anisotropy of crystal structure. Young's modulus with directional dependence for tetragonal

crystals is defined as follows [41]:

$$\frac{1}{E} = S_{11}(a_1^4 + a_2^4) + S_{33}a_3^4 + (2S_{12} + S_{66})a_1^2 a_2^2 + (2S_{13} + S_{44})(a_3^2 - a_3^4) \tag{24}$$

where S_{ij} is the elastic compliance constants, and a_1, a_2 and a_3 are the directional cosines to the X, Y and Z axes, respectively. Fig. 4a illustrates Young's modulus with the directional dependence of YVO$_4$. For an isotropic system, the curved surface should be spherical, while the deviation from the spherical shape indicates the extent of elastic anisotropy. As shown in Fig. 4a, Young's modulus along X, Y and Z axes have greater value, and the 3D surface of YVO$_4$ deviates from the spherical shape largely, which means YVO$_4$ is highly anisotropic. The projections of the 3D surfaces can illustrate the elastic anisotropy more directly and reveal the inter-layer anisotropy, so the projection for YVO$_4$ is analyzed as shown in Fig. 4b. The projection for an isotropic crystal is circular and for YVO$_4$ it deviates from the circular shape significantly. Therefore, YVO$_4$ has a high degree of elastic anisotropy, which is in accordance with the result from the universal elastic anisotropy index analysis.

Hardness, based on the first-principles calculations can be accurately predicted. According to Gao's work [42], the hardness
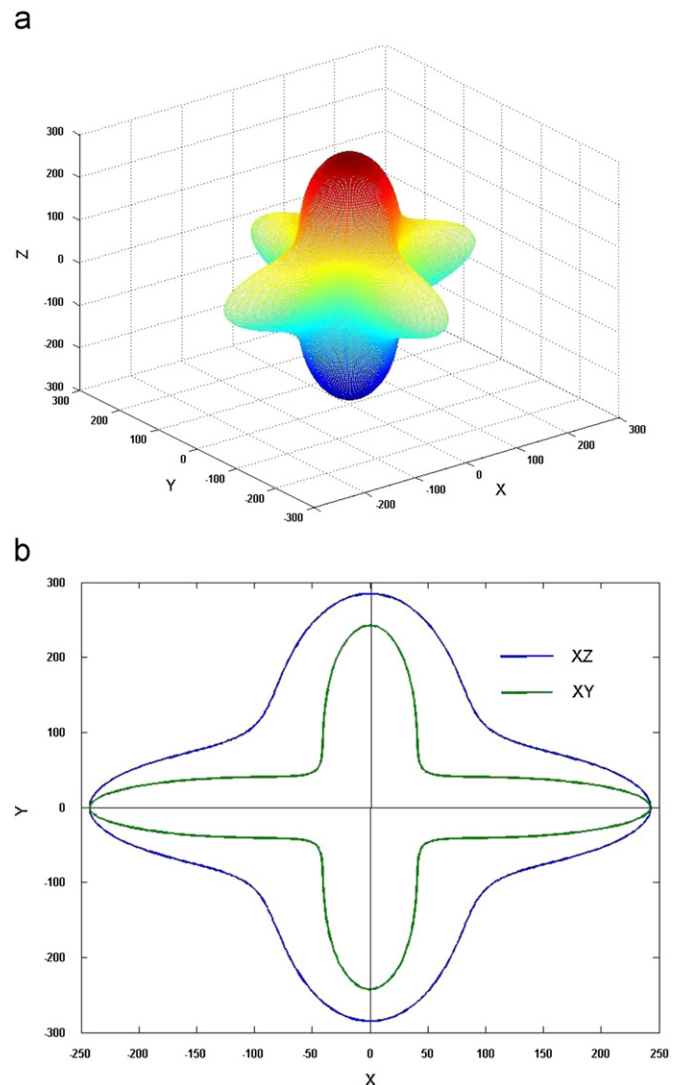

Fig. 4. (a) Directional dependence of Young's modulus in zircon-type YVO$_4$ and (b) projections of the directional dependent Young's modulus in different planes for zircon-type YVO$_4$. The units are in GPa.

Table 2
Bulk modulus B_R, B_V and B_H, shear modulus G_R, G_V and G_H, Young's modulus E (in GPa) and Poisson's ratio v of YVO$_4$.

Method	B_V	B_R	B_H	G_V	G_R	G_H	v	E	B/G	A^U
LDA	150.9	147.1	149.0	65.2	44.1	54.7	0.336	146.2	2.72	2.41
GGA	124.6	120.0	122.3	56.9	44.1	50.5	0.318	133.2	2.42	1.49

of covalent crystals depends on the sum of resistance of each bond per unit volume and can be characterized by average overlap populations. For complex multi-bonding compounds, the hardness of the μ-type bond can be calculated as follows:

$$H_v^\mu(\text{GPa}) = 740 P^\mu (v_b^\mu)^{-5/3} \qquad (25)$$

$$v_b^\mu = \frac{(d^\mu)^3 V_{\text{cell}}}{\sum_v[(d^v)^3 N_b^v]} \qquad (26)$$

where the constant 740 is the proportional coefficient fitted from hardness of diamond, P^μ is the Mulliken overlap population of the μ-type bond, v_b^μ is the volume of a bond of type μ, d^μ is the bond length of type μ, N_b^v is the bond number of type v, V_{cell} is the cell volume of each YVO$_4$ compound. The calculated hardness H_v from Me–O bond of YVO$_4$ is listed in Table 3. For there are no reports on hardness of YVO$_4$ by experiments or calculations, our calculated results can serve as a reference for further investigation. In YVO$_4$, the V–O bonds with shorter bond length and larger Mulliken population make greater contribution to hardness than the Y–O bonds. From the Mulliken population, V cations exhibit electronegativity (0.90 for Al) such that V–O bonds are rather covalent whereas Y cations with high electronegativity (1.46 for Y) generally establish Y–O bonds exhibiting an ionic character.

3.3. Thermodynamic properties

Thermodynamic properties of YVO$_4$ are determined in the temperature range from 0 to 1200 K, where the quasi-harmonic model remains fully valid. The pressure effect is studied in the 0–6 GPa range. The temperature effects on the volume are shown in Fig. 5. The volume increases with increasing temperature. As the pressure increases, the rate of increase becomes a little slower. Fig. 6 presents the relationship of bulk modulus as a function of temperature T up to 1200 K at different pressures. When $T < 200$ K, bulk modulus is nearly a constant, but it drops when $T > 200$ K, which is in accordance with the relationships between volume and temperature as shown in Fig. 5. From the results obtained for the volume and bulk modulus, it appears that the effect of increasing pressure on the material is the same as decreasing temperature of the material.

The investigation on the heat capacity of crystals is an old topic of condensed matter physics with which illustrious names are associated [43]. The heat capacity of a substance not only provides essential insight into its vibrational properties, but is also mandatory for many applications. The heat capacities C_V and C_P versus temperature at 0–6 GPa pressures is shown in Fig. 7a and b. At high temperatures, the constant volume heat capacity C_V tends to the Dulong–Petit limit, which is common to all solids [44]. At sufficiently low temperatures, C_V is proportional to T^3 [45]. At intermediate temperatures, however, the temperature dependence of C_V is governed by the details of vibrations of the atoms and for a long time could only be determined from experiments.

The thermal expansion coefficient α with temperature and pressure for YVO$_4$ is presented in Fig. 8. From Fig. 8 the thermal expansion coefficient α increases with T^3 nearly at low temperatures, gradually the rate becomes gentler, and then approaches a linear increase at high temperatures. The effects of pressure on the thermal expansion

coefficient α are very small at low temperatures; the effects become obvious at high temperature. As pressure increases, the thermal expansion coefficient α decreases. At normal pressure, the linear thermal expansion coefficient of YVO$_4$ from 298 K to 572.5 K is $\alpha_a = 2.2 \times 10^{-6}$/K and $\alpha_c = 8.4 \times 10^{-6}$/K [13], so the thermal expansion for YVO$_4$ is $\alpha = 12.8 \times 10^{-6}$/K. The experimental value of thermal expansion coefficient is very close to the calculated result $\alpha = 13.4 \times 10^{-6}$/K, which means the calculated results are reliable.

4. Conclusions

The physical properties of zircon-type YVO$_4$ are investigated by first-principles calculations. The calculated lattice parameter is
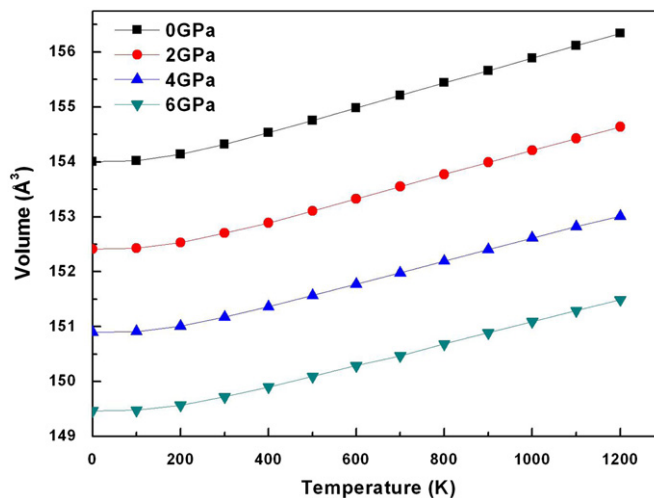

Fig. 5. Relationship between volume and temperature at applied pressures for zircon-type YVO$_4$.
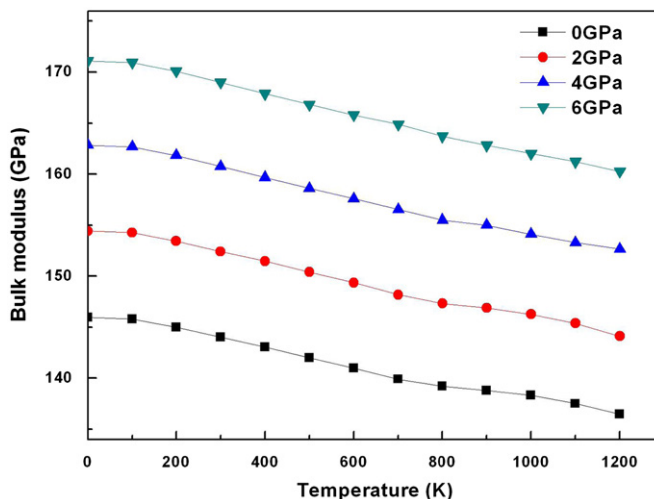

Fig. 6. Relationship between bulk modulus and temperature at applied pressures for zircon-type YVO$_4$.

Table 3
Mulliken population analysis and Hardness of YVO$_4$.

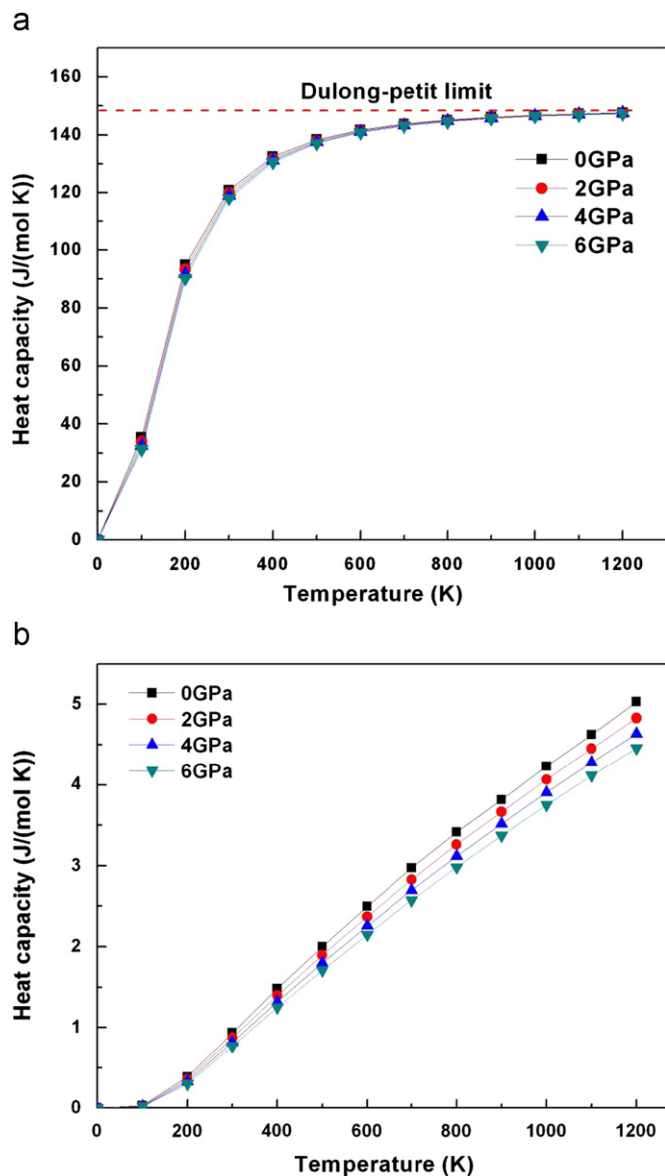| Atom	s	p	d	Total	Charge (e)	Bond	Population	Length (Å)	Nu	Ω (Å^3)	V_b^μ	H_u	H_{Cal}
O	1.85	4.74	0	6.59	−0.59	V–O	0.67	1.69877	8	153.4	4.03	48.64	8.71
V	2.20	6.46	3.44	12.10	0.90	Y–O	0.26	2.26145	8		9.50	4.52	
Y	2.21	6.13	1.20	9.54	1.46		0.08	2.39586	4		11.30	1.04	

Fig. 7. (a) Heat capacity versus temperature at pressures of 0, 2, 4 and 6 GPa and (b) correction, C_P–C_V, due to implicit effects at various pressures.
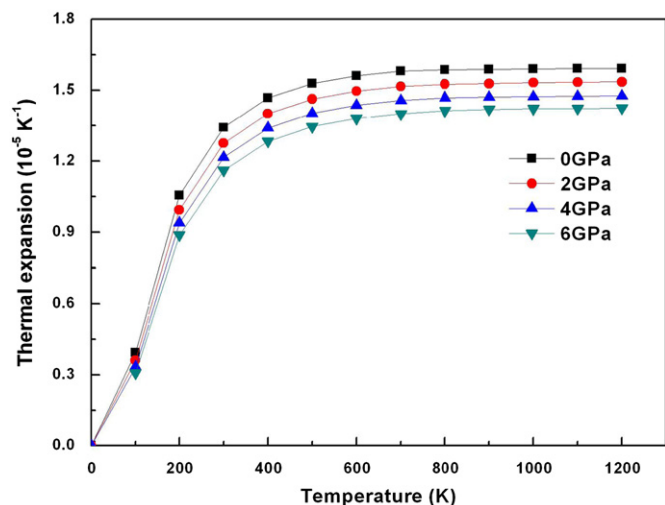

Fig. 8. Thermal expansion versus temperature at pressures of 0, 2, 4 and 6 GPa.

very close to experimental results and other theoretical data. We calculated the total energy of zircon-type YVO_4 at different volumes and modified the E–V relationship by Birch–Murnaghan EOS.

The elastic constants, the aggregate elastic modulus (B, G, E), Poisson's ratio, the anisotropy index and hardness of YVO_4 are also calculated. The calculated elastic constants are in good agreement with experimental and other theoretical results. YVO_4 is mechanically stable due to the mechanical stability criteria for tetragonal structure. According to the critical values for B/G and Poisson's ratio, zircon-type YVO_4 is a kind of ductile material. For YVO_4, V–O bonds make greater contributions to hardness than Y–O.

The thermodynamic properties such as heat capacity and thermal expansion coefficient are predicted using the quasi-harmonic Debye model. It is found that the high temperature leads to a smaller bulk modulus, a larger heat capacity, and a larger thermal expansion coefficient at a given pressure. However, the high pressure results in a larger bulk modulus, a smaller heat capacity and a smaller thermal expansion coefficient at a given temperature. The heat capacity and the thermal expansion coefficient approach to a constant value at high temperatures and high pressures.

Acknowledgments

References

[1] D. Hreniak, J. Doskocz, P. Gluchowski, R. Lisiecki, et al., J. Lumin. 131 (2011) 473.
[2] T. Yasuko, S. Kiyoshi, V.V. Kochurikhin, L.V. Barashov, et al., J. Cryst. Growth 167 (1996) 369.
[3] P.S. Shahid, W.K. Matthew, M.D.C. Lachlan, K.M. Vladimir, et al., Inorg. Chem. 48 (2009) 10553.
[4] J.R. O'Connor, Appl. Phys. Lett. 9 (1966) 407.
[5] P.P. Yaney, L.G. de Shazer, J. Opt. Soc. Am. 66 (1976) 1405.
[6] R.A. Field, M. Birnbaum, C.L. Fincher, Appl. Phys. Lett. 51 (1993) 1025.
[7] J.D. Kinsleg, G.W. Luduig, J. Appl. Phys. 41 (1970) 370.
[8] K. Chow, H.G. Mcknight, Mater. Res. Bull. 8 (1973) 1343.
[9] H.J. Zhang, X.L. Meng, J.H. Liu, L. Zhu, et al., J. Cryst. Growth 216 (2000) 367.
[10] H.J. Cong, H.J. Zhang, B. Yao, W.T. Yu, et al., Cryst. Growth. Des. 10 (2010) 4389.
[11] X. Wang, I. Loa, K. Syassen, M. Hanfland, Phys. Rev. B 70 (2004) 064109.
[12] W. Ruju, L. Fengying, W. Xing, Y. Huangguang, Chin. J. Lasers 27 (2000) 449.
[13] H.J. Zhang, L. Zhu, X.L. Meng, Z.H. Yang, Cryst. Res. Technol. 34 (1999) 1011.
[14] J. Morikawa, C. Leong, T. Hashimoto, T. Ogawa, et al., J. Appl. Phys. 103 (2008) 063522.
[15] M. Oshikiri, M. Boero, A. Matsushita, J.H. Ye, J. Chem. Phys. 131 (2009) 034701.
[16] B.C. Chakoumakos, M.M. Abraham, L.A. Boatner, J. Solid State Chem. 109 (1994) 107.
[17] M.D. Segall, P.J.D. Lindan, M.J. Probert, C.J. Pickard, P.J. Harsnip, S.J. Clark, M.C. Panye, J. Phys.: Condens. Matter 14 (2002) 2717.
[18] D. Vanderbilt, Phys. Rev. B 41 (1990) 7892.
[19] D.M. Ceperley, B.J. Alder, Phys. Rev. Lett. 45 (1980) 566.
[20] J.P. Perdew, Y. Wang, Phys. Rev. B 45 (1992) 13244.
[21] H.J. Monkhorst, J.D. Pack, Phys. Rev. B 13 (1976) 5188.
[22] F. Birch, J. Geophy. Res. 83 (1978) 1257.
[23] J. Zhang, J.Y. Wang, H.J. Zhang, C.L. Wang, et al., J. Appl. Phys. 102 (2007) 023516.
[24] K. Tsubouchi, N. Mikoshiba, IEEE Trans. Sonics Ultrason. Su 32 (1985) 634.
[25] A. Reuss, Z. Angew, Math. Mech. 9 (1929) 49.
[26] O. Beckstein, J.E. Klepeis, G.L.W. Hart, O. Pankratov, Phys. Rev. B 63 (2001) 134112.
[27] M.A. Blanco, E. Franciso, V. Luana, Comput. Phys. Commun. 158 (2004) 7.
[28] A. Boudali, M.D. Khodja, B. Amrani, D. Bourbie, et al., Phys. Lett. A 373 (2009) 879.
[29] H.Z. Fu, D.H. Li, F. Peng, T. Gao, X.L. Cheng, Comp. Mater. Sci. 44 (2008) 774.
[30] Z.C. Huang, J. Feng, W. Pan, Comp. Mater. Sci. 50 (2011) 3056.
[31] M.A. Blanco, A. Martin Pendas, E. Francisco, J.M. Recio, R. Franco, J. Mol. Struct. Theochem. 368 (1996) 45.

[32] E. Francisco, J.M. Recio, M.A. Blanco, A. Martin Pendas, J. Phys. Chem. 102 (1998) 595.
[33] E. Francisco, M.A. Blanco, G. Sanjurjo, Phys. Rev. B 63 (2001) 94107.
[34] R. Hill, Proc. Phys. Soc. Lond. A 65 (1952) 49.
[35] M.W. Stoltzfus, P.M. Woodward, R. Seshadri, J.H. Klepeis, B. Bursten, Inorg. Chem. 46 (2007) 3839.
[36] R.D. Michelle, M.P. Alexandra, W.S. Matthew, C.Y. Samantha, M.W. Patrick, J. Solid State Chem. 182 (2009) 1964.
[37] S.F. Pugh, Phil. Mag. 45 (1954) 823.

[38] P. Ravindran, L. Fast, P.A. Korzhavyi, B. Johansson, J. Wills, O. Eriksson, J. Appl. Phys. 84 (1998) 4891.
[39] C. Zener, Elasticity and Anelasticity of Metals, University of Chicago, Chicago, 1948.
[40] I.R. Shivakumar, O.S. Martin, Phys. Rev. Lett. 101 (2008) 055504.
[41] J.F. Nye, Physical Properties of Crystals, Clarendon Press, Oxford, 1964.
[42] F.M. Gao, Phys. Rev. B 73 (2006) 132104.
[43] A. Einstein, Ann. Phys. 22 (1907) 80.
[44] A.T. Petit, P.L. Dulong, Ann. Chim. Phys. 10 (1819) 95.
[45] P. Debye, Ann. Phys. 39 (1912) 89.